

# Leptonic CP violation studies at M in iBooNE in the (3+2) sterile neutrino oscillation hypothesis

G. K aragiorgi, A. A guilar-A revalo,<sup>y</sup> J. M. C onrad,<sup>z</sup> and M. H. S haevitz<sup>x</sup>  
D epartment of P hysics, C olumbia U niversity, N ew Y ork, N Y 10027

K. W hisnant<sup>t</sup>  
D epartment of P hysics and A stronomy, I owa S tate U niversity, A mes, I A 50011

M. S orei  
I nstituto de F isica C orpuscular, I FIC, C SIC and U niversidad de V alencia, S pain

V. B arger<sup>yy</sup>  
D epartment of P hysics, U niversity of W isconsin, M adison, W I 53715  
(D ated: M ay 25, 2019)

We investigate the extent to which leptonic CP violation in (3+2) sterile neutrino models leads to different oscillation probabilities for  $\nu_e$  and  $\bar{\nu}_e$  oscillations at M in iBooNE. We are using a combined analysis of short-baseline (SBL) oscillation results, including the LSND and null SBL results, to which we impose additional constraints from atmospheric oscillation data. We obtain the favored regions in M in iBooNE oscillation probability space for both (3+2) CP-conserving and (3+2) CP-violating models. We further investigate the allowed CP-violation phase values and the M in iBooNE reach for such a CP violation measurement. The analysis shows that the oscillation probabilities in M in iBooNE neutrino and antineutrino running models can differ significantly, with the latter possibly being as much as three times larger than the first. In addition, we also show that all possible values of the single CP-violation phase measurable at short baselines in (3+2) models are allowed within 99% CL by existing data.

PACS numbers: 14.60.Pq, 14.60.St, 12.15.Ff

## I. INTRODUCTION

One of the most pressing open questions in neutrino physics today is whether or not leptons conserve the fundamental CP symmetry. The consequences of leptonic CP symmetry violation would be far-reaching and extend beyond the realm of particle physics, possibly being related to the matter-antimatter asymmetry observed in the Universe today [1].

In the standard paradigm of three-active-neutrino mixing occurring at the solar [2, 3, 4, 5, 6, 7, 8] and atmospheric [9, 10, 11, 12, 13] oscillation scales only, leptonic CP violation would yield different vacuum oscillation probabilities for neutrinos and antineutrinos that could be observed, for example, with accelerator-based neutrino oscillation appearance experiments operating near the atmospheric oscillation maximum [14, 15]. This is because CP-odd terms in the oscillation probability formula would appear from solar/atmospheric interference terms involving the single CP-violating Dirac phase

appearing in the neutrino mixing matrix [16].

Neutrino models involving active/sterile neutrino mixing [17] at the LSND [18] neutrino mass splitting scale via at least two sterile neutrino states [19, 20] would open the possibility for further manifestations of leptonic CP violation, including ones that could be measurable with neutrino appearance experiments at short baselines also. In this paper, we investigate short-baseline (SBL) leptonic CP violation in (3+2) sterile neutrino models. A schematic diagram describing (3+2) sterile neutrino models is shown in Fig. 1.

The analysis uses the same seven SBL datasets as in Ref. [20], including results on  $\nu_e$  disappearance (from the CCFR 84 [21] and C D H S [22] experiments),  $\bar{\nu}_e$  disappearance (from the Bugey [23] and C H O O Z [24] experiments), and  $\nu_e$  oscillations (from the LSND [18], K A R - M E N 2 [25], and N O M A D [26] experiments). In addition, additional atmospheric constraints have been added to the combined fit, based on the analysis of Ref. [27].

Based on the combined analysis of the above SBL and atmospheric oscillation data, we estimate the range of fundamental neutrino parameters in (3+2) sterile neutrino models that are allowed within the experimental capabilities of M in iBooNE, following a similar analysis to that in Ref. [20]. However, in this case, the CP conservation requirement is relaxed, allowing for different neutrino and antineutrino oscillation probabilities.

The paper is organized as follows. In Section II, we specify the neutrino oscillation formalism used in this

E lectronic address: georgia@nevis.columbia.edu

<sup>y</sup>E lectronic address: alexis@phys.columbia.edu

<sup>z</sup>E lectronic address: conrad@nevis.columbia.edu

<sup>x</sup>E lectronic address: shaevitz@nevis.columbia.edu

<sup>t</sup>E lectronic address: whisnant@iastate.edu

E lectronic address: sorei@i.c.uv.es

<sup>yy</sup>E lectronic address: barger@physics.wisc.edu

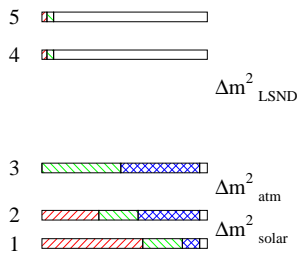


FIG. 1: Flavor content of neutrino mass eigenstates in (3+2) models. Neutrino masses increase from bottom to top. The  $\nu_e$  fractions are indicated by red (right-leaning) hatches, the  $\nu_\mu$  fractions by green (left-leaning) hatches, the  $\nu_\tau$  fractions by blue crosshatches, and the  $\nu_s$  fractions by no hatches. The flavor contents shown are schematic only. [20]

analysis to describe (3+2), CP-violating neutrino oscillations. In Section III, we discuss the analysis followed in this paper, used to constrain neutrino oscillation parameters with short-baseline and atmospheric data. In Section IV, we present the results obtained for the CP-conserving, and CP-violating (3+2) models. For both cases, we explore the oscillation probability space experimentally allowed in MINIBoONE, and we quote the neutrino mass and mixing parameters for the best-fit models derived from the combined SBL+atmospheric constraint analysis. In Section V, we discuss the constraints on the single CP-violation phase that could be measured at short baselines, inferred from a CP-violating (3+2) analysis of SBL+atmospheric oscillation results, and how the MINIBoONE CP asymmetry observable is expected to vary as a function of this CP-violation phase.

## II. INCLUDING CP VIOLATION IN THE STERILE NEUTRINO OSCILLATION FORMALISM

In the sterile neutrino oscillation formalism, under the assumptions of CPT invariance, the probability for a neutrino produced with flavor and energy  $E$ , to be detected as a neutrino of flavor after travelling a distance  $L$ , is [28, 29]:

$$P(\nu_i \rightarrow \nu_j) = \frac{4}{2} \sum_{i,j}^P R(U_{ij} U_{ij}^* U_{ij} U_{ij}^*) \sin^2 x_{ij} + \frac{4}{2} \sum_{i,j}^P I(U_{ij} U_{ij}^* U_{ij} U_{ij}^*) \sin 2x_{ij} \quad (1)$$

where  $R$  and  $I$  indicate the real and imaginary parts of the product of mixing matrix elements, respectively;  $i, e; \mu, \tau$ , or  $s$ , ( $s$  being the sterile flavor);  $i, j = 1, \dots, N$  ( $N$  being the number of neutrino species); and  $x_{ij} = 1.27 m_{ij}^2 L / E$ . In defining  $x_{ij}$ , we take the neutrino mass splitting  $m_{ij}^2 = m_i^2 - m_j^2$  in  $\text{eV}^2$ , the neutrino baseline  $L$  in  $\text{km}$ , and the neutrino energy  $E$  in  $\text{GeV}$ . For antineutrinos, the oscillation probability is obtained from Eq. 1 by replacing the mixing matrix  $U$  with its complex

conjugate matrix. Therefore, if the mixing matrix is not real, neutrino and antineutrino oscillation probabilities can differ.

For  $N$  neutrino species, there are, in general,  $(N-1)$  independent mass splittings,  $N(N-1)=2$  independent moduli of parameters in the unitary mixing matrix, and  $(N-1)(N-2)=2$  Dirac CP-violating phases that may be observed in oscillations.

In SBL neutrino experiments that are sensitive only to  $\nu_e \rightarrow \nu_e$ ,  $\nu_\mu \rightarrow \nu_\mu$ , and  $\nu_\tau \rightarrow \nu_\tau$  transitions, the set of observable parameters is reduced considerably. Firstly, oscillations due to atmospheric and solar mass splittings can be neglected in this case, or equivalently one can set  $m_1 = m_2 = m_3$ . Secondly, mixing matrix elements that measure the neutrino flavor fraction of the various neutrino mass eigenstates do not enter in the oscillation probability. In this case, the number of observable parameters is restricted to  $(N-3)$  independent mass splittings,  $2(N-3)$  moduli of mixing matrix parameters, and  $(N-3)(N-4)=2$  CP-violating phases. Therefore, for (3+2) sterile neutrino models depicted in Fig. 1, that is for the  $N=5$  case, there are two independent mass splittings  $m_{41}^2$  and  $m_{51}^2$ , four moduli of mixing matrix parameters  $U_{e4}^2$ ,  $U_{4\bar{e}}^2$ ,  $U_{e5}^2$ ,  $U_{5\bar{e}}^2$  and one CP-violating phase. The convention used in the following for this CP-phase is:

$$\phi_{45} = \arg(U_{e5} U_{4\bar{e}} U_{45} U_{e4}) \quad (2)$$

Under these assumptions, the general oscillation formula in Eq. 1 can be rewritten as:

$$P(\nu_i \rightarrow \nu_j) = 1 - 4[(1 - U_{4\bar{e}}^2 - U_{5\bar{e}}^2) + (U_{4\bar{e}}^2 \sin^2 x_{41} + U_{5\bar{e}}^2 \sin^2 x_{51}) + U_{4\bar{e}}^2 U_{5\bar{e}}^2 \sin^2 x_{54}] \quad (3)$$

and

$$P(\nu_i \rightarrow \bar{\nu}_j) = 4U_{4\bar{e}}^2 U_{4\bar{e}}^* \sin^2 x_{41} + 4U_{5\bar{e}}^2 U_{5\bar{e}}^* \sin^2 x_{51} + 8U_{4\bar{e}} U_{5\bar{e}} U_{4\bar{e}}^* U_{5\bar{e}}^* \sin x_{41} \sin x_{51} \cos(x_{54} + \phi_{45}) \quad (4)$$

for  $\phi_{45} = \phi$  and  $\phi_{54} = \epsilon$ , respectively. The formulas for antineutrino oscillations are obtained by substituting  $\phi_{45} = -\phi_{45}$ .

## III. ANALYSIS METHOD

The analysis we perform is a combined SBL+atmospheric analysis, with the purpose of obtaining the (3+2) model allowed regions in oscillation probability space for neutrino and antineutrino running modes expected at MINIBoONE, and the allowed values of the CP-violation phase  $\phi_{45}$ . The physics and statistical assumptions used in the analysis to describe the SBL experiments closely follow the ones described in detail in Ref. [20]. The Monte

Carlo method used to apply the oscillation formalism discussed in Section II also closely follows the one described in Ref. [20]. The full set of oscillation parameters ( $m_{41}^2; U_{e4}^2; U_{45}^2; m_{51}^2; U_{e5}^2; U_{54}^2$ ) is allowed to freely vary, constrained only by: 1)  $0.1\text{eV}^2 < m_{41}^2; m_{51}^2 < 100\text{eV}^2$ , with  $m_{51}^2 = m_{41}^2$ , for definiteness; and 2)  $U_{e1}^2 + U_{13}^2 = 0.5$ , and  $U_{43}^2 + U_{53}^2 = 0.5$ . The first constraint defines the higher  $m^2$  splitting range considered, imposed by the LSND signature, whereas the second constraint requires the fourth and fifth mass eigenstates to include only small active flavor quantities, as suggested by the solar and atmospheric oscillation data.

A slight modification was made to the analysis method used in this paper, compared to the one used in Ref. [20]. Rather than generating neutrino masses and mixings in a random, unbiased way, we use importance sampling via a Markov chain Monte Carlo method [30, 31], to better sample the regions in parameter space that provide a good fit to the SBL+atmospheric data. Given a starting point (model)  $x_i$  in the ( $m_{41}^2; U_{e4}^2; U_{45}^2; m_{51}^2; U_{e5}^2; U_{54}^2$ ) parameter space, a trial state  $x_{i+1} = x_i + e$  that depends only on the current state  $x_i$  and on the probability distribution function for the random vector  $e$ , is generated. The probability for the trial state  $x_{i+1}$  to be accepted as the new current state for further model random generation is given by the transition probability:

$$P(x_i \rightarrow x_{i+1}) = \min\{1, \exp[-(x_{i+1}^2 - x_i^2)/T]\} \quad (5)$$

where  $\frac{2}{i}$  and  $\frac{2}{i+1}$  are  $\chi^2$  values for the states  $x_i$  and  $x_{i+1}$ , quantifying the agreement between the models and the short-baseline plus atmospheric results used in the combined analysis, and  $T$  is an effective "temperature" parameter. The results presented here are obtained by combining various Markov chains with different initial conditions, probability distribution functions for  $e$ , and temperature parameters. This modification allows for an efficient probe of the larger dimensionality of the parameter set present in CP-violating models, compared to CP-conserving models.

The addition of atmospheric constraints to our previous analysis [20] follows the assumptions discussed in Ref. [27]. These constraints include 1489 days of Super-Kamokande charged-current data [9], including the electron-like and muon-like data samples of sub- and multi-GeV contained events, stopping events, and through-going upgoing muon data events. The analysis in Ref. [27] assumes the three-dimensional atmospheric neutrino fluxes given in [32], and a treatment of flux, cross-section, and experimental systematic uncertainties given in [33]. The atmospheric constraint includes also data on disappearance from the long baseline, accelerator-based experiment K2K [13]. The atmospheric constraint is implemented in our analysis by simply adding a contribution  $\chi^2_{\text{atm}} = \chi^2_{\text{atm}}(d)$  to the total SBL contribution,  $\chi^2_{\text{SBL}} = \chi^2_{\text{SBL}}(m_{41}^2; U_{e4}^2; U_{45}^2; m_{51}^2; U_{e5}^2; U_{54}^2)$ ,

where:

$$d = \frac{1 - \frac{P}{1 - 4A}}{2} \quad (6)$$

with:

$$A = (1 - U_{43}^2 - U_{53}^2)(U_{43}^2 + U_{53}^2) + U_{43}^2 U_{53}^2 \quad (7)$$

and by consequently adding a single degree of freedom to our analysis. We note that the recent analysis of atmospheric K2K data in Ref. [27] constrain the quantity  $d$  in Eq. 6, and therefore muon neutrino disappearance at the LSND mass splitting scale, significantly more than previous results. For reference, the authors of Ref. [27] quote an upper limit on  $d$  of 0.065 at 99% CL, while  $d = 0.13$  at 99% CL is given in Ref. [34].

The combined  $\chi^2$  used to extract the best-fit values and allowed ranges for the fundamental oscillation parameters  $m_{41}^2, m_{51}^2, U_{e4}, U_{45}, U_{e5}, U_{54}$ , given in Sections IV and V, is therefore:

$$\chi^2_{\text{SBL}} + \chi^2_{\text{atm}} \quad (8)$$

In CP-conserving models,  $U_{45}$  is only allowed to take values of 0, or 1, whereas in CP-violating models,  $U_{45}$  can vary within the full  $(0; 1)$  range. Inclusion of this additional parameter reduces the total number of degrees of freedom by one.

This analysis also provides realistic estimates of the oscillation probabilities to be expected in MiniBooNE in the framework of allowed CP-conserving and CP-violating (3+2) sterile neutrino models. For that, expected neutrino transmutation rates for full  $\nu_e \rightarrow \bar{\nu}_e$  or

$\bar{\nu}_e \rightarrow \nu_e$  transmutations as a function of neutrino or anti-neutrino energy are considered, for neutrino and anti-neutrino running modes in MiniBooNE. These distributions are weighted according to the oscillation probability formula in Eq. 4 to estimate the number of oscillation signal events for any (3+2) model, prior to event reconstruction and particle identification. The predictions for the full transmutation rates are obtained by multiplying the flux distributions as a function of energy for muon neutrinos and antineutrinos in both neutrino and antineutrino running modes (four flux distributions in total) by the (energy-dependent) total electron neutrino and antineutrino cross-sections on  $\text{CH}_2$ , respectively. The flux predictions are obtained from a full simulation of the FNAL Booster neutrino beam line [35], while the neutrino cross-section predictions are obtained from the NUAICE event generator [36]. We do, therefore, take into account also the effect of "wrong sign" neutrinos in computing the expected oscillation probabilities, which have the effect of washing out CP-violating observables. This effect is non-negligible since as much as one third of the total interaction rate in antineutrino running mode is expected to be due to neutrinos rather than antineutrinos; on the other hand, the antineutrino contribution in neutrino running mode is expected to be much smaller.

#### IV. OSCILLATION PROBABILITY EXPECTATIONS FOR M IN iBOONE

We define the oscillation probability in neutrino (antineutrino) mode expected at M in iBoone as:

$$p_{\text{BooNE}} = \frac{R \int dE [p(-\theta_e) N_0(\theta) + p(+\theta_e) N_0(\theta)]}{R \int dE [N_0(\theta) + N_0(\theta)]} \quad (9)$$

where  $E$  is the neutrino energy;  $p(-\theta_e)$  and  $p(+\theta_e)$  are the oscillation probabilities given by Eq. 4, with  $\theta_{45} = 0$  or  $\pi$  for the CP-conserving case, and  $0 < \theta_{45} < 2\pi$  for the CP-violating case;  $N_0(\theta)$  and  $N_0(\theta)$  are the M in iBoone neutrino and antineutrino full-transmutation rate distributions in neutrino running mode, and  $N_0(\theta)$  and  $N_0(\theta)$  are the neutrino and antineutrino full-transmutation rate distributions in antineutrino running mode, as defined in Section III.

This section consists of two parts. In the first part, we explore the oscillation probability allowed regions  $(p_{\text{BooNE}}; p_{\text{BooNE}})$  at 90% and 99% CL obtained from the SBL+atm ospheric analysis, assuming (3+2) CP-conserving models. In the second part, we explore the same parameter space  $(p_{\text{BooNE}}; p_{\text{BooNE}})$  for (3+2) CP-violating models. In both parts, we quote the values for the masses and mixing parameters corresponding to the best-fit models in the  $(p_{\text{BooNE}}; p_{\text{BooNE}})$  space.

The 90%, and 99% CL allowed region are defined as the  $(p_{\text{BooNE}}; p_{\text{BooNE}})$  space for which  $\chi^2_{\text{min}} < 4.61$ , and  $\chi^2_{\text{min}} < 9.21$ , respectively, where  $\chi^2_{\text{min}}$  is the absolute  $\chi^2$  minimum for all  $(p_{\text{BooNE}}; p_{\text{BooNE}})$  values.

##### A. CP-conserving models results

Fig. 2 shows predictions for the oscillation probabilities expected in M in iBoone neutrino and antineutrino modes, in the CP-conserving, (3+2) sterile neutrino hypothesis. The bottom left panel in Fig. 2 shows the region in  $(p_{\text{BooNE}}; p_{\text{BooNE}})$  space that is allowed at the 90% and 99% confidence level (2 dof) by existing short-baseline data used in the analysis, including LSND. The star indicates the best-fit, at  $p_{\text{BooNE}} = p_{\text{BooNE}} = 0.13 \times 10^{-2}$ . The effect of "fake" CP-violation due to spectrum differences in neutrino and antineutrino running modes manifests itself as a departure from the dotted line in the bottom left panel of Fig. 2. The effect is at the few percent level at most.

The top left and bottom right panels in Fig. 2 show the 1-dimensional projections of the  $\chi^2$  contours obtained from the SBL+atm ospheric data, as a function of  $p_{\text{BooNE}}$  and  $p_{\text{BooNE}}$ , respectively. The dashed lines at  $\chi^2 = 2.70$  and  $6.63$  indicate the 90% and 99% CL regions, respectively (1 dof). M in iBoone is expected to measure an oscillation probability in excess of  $> 0.05 \times 10^{-2}$  if CP-conserving (3+2) models are correct.

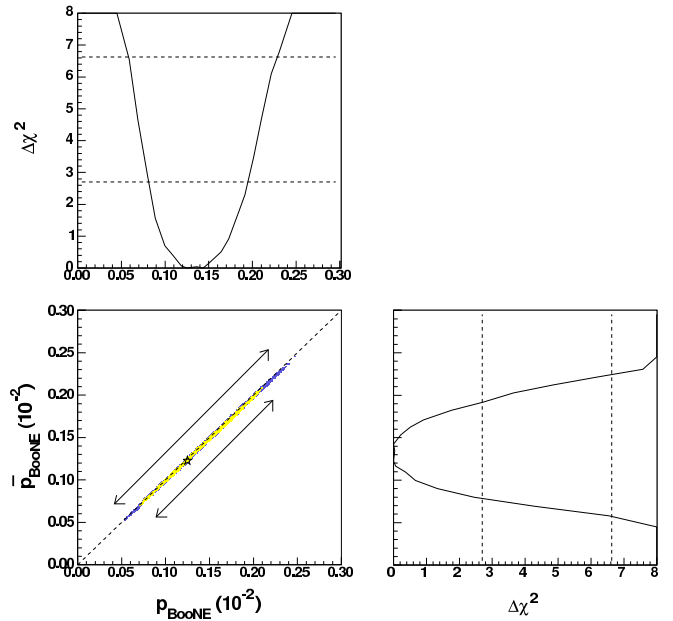


FIG. 2: Expected oscillation probabilities at M in iBoone in neutrino and antineutrino running modes, for CP-conserving (3+2) models. The yellow (light grey) region corresponds to the 90% CL allowed region; the blue (dark grey) region corresponds to the 99% CL allowed region. Two arrows, one for each confidence level, have been drawn in the Figure to guide the eye to the location of the narrow allowed regions. See text for details.

The best-fit model parameters for CP-conserving (3+2) sterile neutrino oscillation models are shown in Table I.

##### B. CP-violating models results

Fig. 3 shows the order of magnitude of the CP-violating effects to be expected in  $(p_{\text{BooNE}}; p_{\text{BooNE}})$  space, as  $\theta_{45}$  is varied over its allowed range  $(0; 2\pi)$ , while the remaining oscillation parameters are fixed to their best-fit values for the CP-conserving case. In this particular Figure, where we neglect goodness-of-fit considerations of the SBL+atm ospheric datasets as a function of  $\theta_{45}$  variations, neutrino/antineutrino oscillation probability differences as large as a factor of two can be obtained, near maximal CP-violation ( $\theta_{45} = \pi/2$  or  $3\pi/2$ ). As will be seen below, a similar conclusion (with actually even larger differences allowed among neutrino and antineutrino running modes) is reached with a more quantitative analysis that takes into account  $\theta_{45}$  variations as a function of all neutrino parameters.

Fig. 4 shows the oscillation probabilities to be expected at M in iBoone in neutrino and antineutrino running modes, in a CP-violating, (3+2) scenario.

Unlike in Fig. 3, in Fig. 4 all parameters ( $m_{41}^2, m_{51}^2, \Delta m_{41}^2, \Delta m_{45}^2, \Delta m_{51}^2, \theta_{45}$ ) are now allowed

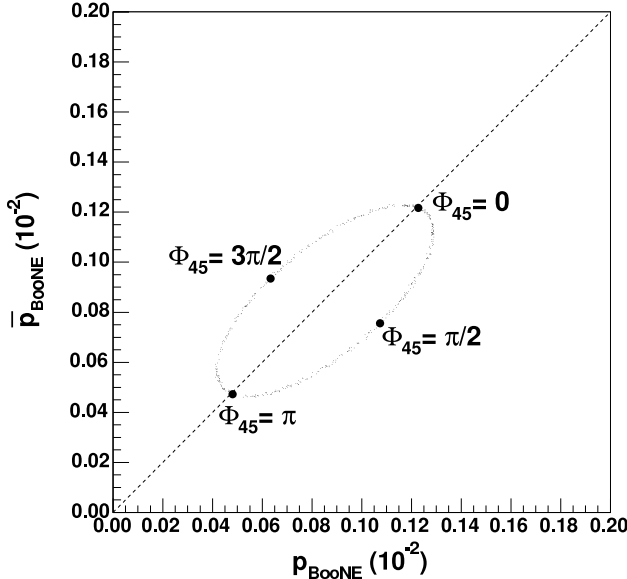


FIG. 3: Illustration of expected oscillation probabilities at M in iBooNE in neutrino and antineutrino running modes, for CP-violating (3+2) models with atmospheric constraint. Here, the neutrino masses and mixings are fixed to their best-fit values and the only parameter that is allowed to vary is the CP-violating phase,  $\Phi_{45}$ .

Model	$\chi^2$ (d.o.f.)	$m_{41}^2$	$m_{51}^2$	$\mathcal{U}_{e4j}$	$\mathcal{U}_{4j}$	$\mathcal{U}_{e5j}$	$\mathcal{U}_{5j}$	$\Phi_{45}$
CPC	141.4 (145)	0.92	24	0.132	0.158	0.066	0.159	0
CPV	140.8 (144)	0.91	24	0.127	0.147	0.068	0.164	1.8

TABLE I: Comparison of best-fit values for mass splittings and mixing parameters for (3+2) CP-conserving and CP-violating models. Mass splittings are shown in  $\text{eV}^2$ . See text for details.

to vary within the constraints provided by existing SBL+atmospheric oscillation results. Compared to the CP-conserving case of Fig. 2, the best-fit point (indicated by a star) does not change significantly; however, large asymmetries due to CP-violation are now possible, shown by departures from the dashed line in the bottom-left panel of Fig. 4. The general trend is that the 2-dimensional allowed region in  $(P_{\text{BooNE}}, \bar{P}_{\text{BooNE}})$  space is tilted more horizontally compared to the dashed line  $P_{\text{BooNE}} = \bar{P}_{\text{BooNE}}$ , indicating that existing short-baseline results constrain more  $\Phi_{45}$  than  $\Phi_{45}$  oscillations.

The best-fit model parameters for CP-violating (3+2) sterile neutrino oscillation models are shown in Table I. From a comparison of the  $\chi^2$  values given in the Table, it is clear that CP-violating, (3+2) models do not provide a significantly better description of short-baseline and atmospheric data, compared to CP-conserving, (3+2) models.

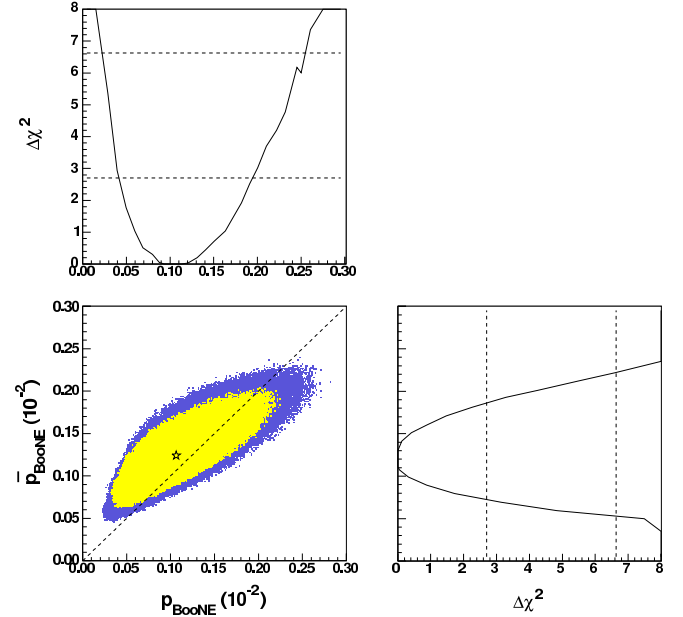


FIG. 4: Expected oscillation probabilities at M in iBooNE in neutrino and antineutrino running modes, for CP-violating (3+2) models. The yellow (light grey) region corresponds to the 90% CL allowed region; the blue (dark grey) region corresponds to the 99% CL allowed region. See text for details.

## V. CONSTRAINTS ON CP-VIOLATION PHASE

In this section we discuss the present constraints on the short-baseline, CP-violating phase  $\Phi_{45}$  that the current SBL+atmospheric oscillation data impose on (3+2) sterile neutrino oscillation models, and the prospects of observing such phase at M in iBooNE. From the M in iBooNE appearance measurements in neutrino and antineutrino running modes, the following CP asymmetry observable,  $A_{CP}$ , can be extracted:

$$A_{CP} = \frac{P_{\text{BooNE}} - \bar{P}_{\text{BooNE}}}{P_{\text{BooNE}} + \bar{P}_{\text{BooNE}}} \quad (10)$$

The top-left panel in Fig. 5 shows that all values for the CP-phase  $\Phi_{45}$  are presently allowed at the 99% confidence level, and that CP-violating, (3+2) models with small degrees of CP violation are marginally preferred. The bottom-left plot shows that large CP asymmetry is possible, but not required, for maximal CP-violation, given by phases of around  $\Phi_{45} = -2$  and  $3 = 2$ . In particular, CP asymmetries up to  $A_{CP} = 0.5$  could be obtained, corresponding to a three times larger oscillation probability in antineutrino running mode, compared to the neutrino running mode probability.

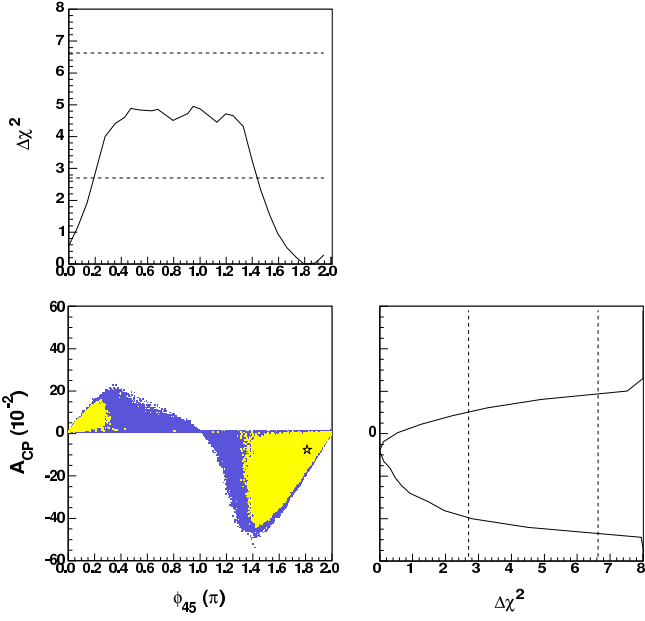


FIG. 5: Current limits on the CP-violating phase  $\Phi_{45}$  from current short-baseline results, and CP asymmetry measurement expected at M inBooNE,  $A_{CP}$ , as a function of  $\Phi_{45}$ . The yellow (light grey) region corresponds to the 90% CL allowed region; the blue (dark grey) region corresponds to the 99% CL allowed region. See text for details.

## VI. CONCLUSIONS

We have performed a combined analysis of data from seven short-baseline experiments (Bugey, CHOOZ, CCFR 84, CDHS, KARMEN, LSND, NOMAD), and including also constraints from atmospheric oscillation data (Super-Kamiokande, K2K), for the (3+2) neutrino oscillation hypothesis, with two sterile neutrinos at high  $m^2$ . The motivation for considering two light, sterile neutrino models arises from the tension in trying to reconcile, in a CPT-conserving framework, the LSND signal for oscillations with the null results obtained by the other SBL experiments with a single light sterile neutrino state [20, 37, 38, 39]. The class of (3+2) sterile neutrino models open up the possibility of observing possible leptonic CP-violating effects at short-baseline experiments, and in particular within the experimental capabilities of M inBooNE.

We have described two types of analyses in the (3+2) neutrino oscillation hypothesis. In the first analysis, we treat the SBL datasets with additional atmospheric constraints in a CP-conserving scenario, and we determine the allowed oscillation probabilities at M inBooNE in both neutrino and antineutrino running modes, as well as the best-fit values for the mass splittings and mixing parameters. In the second analysis, we consider a CP-violating scenario to obtain the favored regions in M inBooNE oscillation probability space, we determine

the best-fit values for the mass splittings and mixing parameters, and we further investigate the allowed CP-violating phase values, quoting the best-fit value for the CP-violating phase.

The main results of the analysis are given in Sections IV and V. First, we find that CP-violating, (3+2) models do not provide a significantly better description of short-baseline and atmospheric data, compared to CP-conserving, (3+2) models. On the other hand, even if only a small degree of CP violation is marginally preferred, we also find that existing data allow for all possible values for the single CP-violating phase that could be observed at short baselines in (3+2) models, at 99% CL. Finally, if leptonic CP violation occurs and (3+2) sterile neutrino models are a good description of the data, we find that differences as large as a factor of three between the electron (anti-)neutrino appearance probabilities in neutrino and antineutrino running modes at M inBooNE are possible.

The existence of a fifth neutrino with mass of order 5 eV, as found in our fits, would be in conflict with cosmological bounds obtained under the assumption that all the neutrinos are in thermal equilibrium, see, e.g., [40]. However, these bounds may be avoided if the neutrinos do not thermalize [41] or if the reheating temperature of the universe is very low [42].

## Acknowledgments

We thank O. Yasuda for useful suggestions, M. Maltoni for providing the data on atmospheric constraints, the M inBooNE Collaboration for providing the neutrino flux and cross-section expectations for the M inBooNE experiment, and K. Abazajian for introducing one of us (MS) to Markov chain Monte Carlo simulations. This work was supported by NSF grant no. PHY-0500492, by U.S. Dept. of Energy grant nos. DE-FG 02-95ER 40896 and DE-FG 02-01ER 41155, by the Wisconsin Institute for Research Foundation, and by a Marie Curie Intra-European Fellowship within the 6th European Framework Program.

---

[1] A. D. Sakharov, *Pisma Zh. Eksp. Teor. Fiz.* 5, 32 (1967) [*JETP Lett.* 5, 24 (1967) *SO PUA*, 34, 392–393.1991 *UFNAA*, 161, 61–64.1991].

[2] B. T. Cleveland et al., *Astrophys. J.* 496, 505 (1998).

[3] Y. Fukuda et al. [Super-Kamiokande Collaboration], *Phys. Rev. Lett.* 81, 1158 (1998) [erratum *ibid.* 81, 4279 (1998)] [[arXiv:hep-ex/9805021](#)]; *Phys. Rev. Lett.* 82, 2430 (1999) [[arXiv:hep-ex/9812011](#)].

[4] J. N. Abdurashitov et al. [SAGE Collaboration], *J. Exp. Theor. Phys.* 95, 181 (2002) [*Zh. Eksp. Teor. Fiz.* 122, 211 (2002)] [[arXiv:astro-ph/0204245](#)].

[5] W. Hampel et al. [GALLEX Collaboration], *Phys. Lett. B* 447, 127 (1999).

[6] M. A. Immann et al. [GNO Collaboration], *Phys. Lett. B* 490, 16 (2000) [[arXiv:hep-ex/0006034](#)].

[7] Q. R. Ahmad et al. [SNO Collaboration], *Phys. Rev. Lett.* 89, 011301 (2002) [[arXiv:nucl-ex/0204008](#)]; *Phys. Rev. Lett.* 89, 011302 (2002) [[arXiv:nucl-ex/0204009](#)]; *Phys. Rev. Lett.* 87, 071301 (2001) [[arXiv:nucl-ex/0106015](#)].

[8] T. Araki et al. [KamLAND Collaboration], *Phys. Rev. Lett.* 94, 081801 (2005) [[arXiv:hep-ex/0406035](#)].

[9] Y. Fukuda et al. [Super-Kamiokande Collaboration], *Phys. Lett. B* 433, 9 (1998) [[arXiv:hep-ex/9803006](#)]; *Phys. Lett. B* 436, 33 (1998) [[arXiv:hep-ex/9805006](#)]; *Phys. Rev. Lett.* 81, 1562 (1998) [[arXiv:hep-ex/9807003](#)]; *Phys. Rev. Lett.* 82, 2644 (1999) [[arXiv:hep-ex/9812014](#)]; *Phys. Lett. B* 467, 185 (1999) [[arXiv:hep-ex/9908049](#)]; Y. Ashie et al. [Super-Kamiokande Collaboration], *Phys. Rev. D* 71, 112005 (2005) [[arXiv:hep-ex/0501064](#)].

[10] D. Casper et al., *Phys. Rev. Lett.* 66, 2561 (1991); R. Becker-Szendy et al., *Phys. Rev. Lett.* 69, 1010 (1992).

[11] M. Ambrosio et al. [MACRO Collaboration], *Phys. Lett. B* 434, 451 (1998) [[arXiv:hep-ex/9807005](#)]; *Phys. Lett. B* 478, 5 (2000) [[arXiv:hep-ex/0001044](#)]; *Phys. Lett. B* 517, 59 (2001) [[arXiv:hep-ex/0106049](#)]; *Phys. Lett. B* 566, 35 (2003) [[arXiv:hep-ex/0304037](#)].

[12] W. W. M. Allison et al., *Phys. Lett. B* 391, 491 (1997) [[arXiv:hep-ex/9611007](#)]; *Phys. Lett. B* 449, 137 (1999) [[arXiv:hep-ex/9901024](#)]; M. C. Sanchez et al. [Soudan 2 Collaboration], [[arXiv:hep-ex/0307069](#)].

[13] S. H. Ahn et al. [K2K Collaboration], *Phys. Lett. B* 511, 178 (2001) [[arXiv:hep-ex/0103001](#)]; *Phys. Rev. Lett.* 90, 041801 (2003) [[arXiv:hep-ex/0212007](#)]; [[arXiv:hep-ex/0606032](#)].

[14] V. Barger, D. Marfatia and K. Whisnant, *Int. J. Mod. Phys. E* 12, 569 (2003) [[arXiv:hep-ph/0308123](#)].

[15] O. Mena, *Mod. Phys. Lett. A* 20, 1 (2005) [[arXiv:hep-ph/0503097](#)].

[16] V. D. Barger, K. Whisnant and R. J. N. Phillips, *Phys. Rev. Lett.* 45, 2084 (1980).

[17] J. J. Gomez-Cadenas and M. C. Gonzalez-Garcia, *Z. Phys. C* 71, 443 (1996) [[arXiv:hep-ph/9504246](#)].

[18] C. Athanassopoulos et al. [LSND Collaboration], *Phys. Rev. Lett.* 77, 3082 (1996) [[arXiv:nucl-ex/9605003](#)]; *Phys. Rev. C* 58, 2489 (1998) [[arXiv:nucl-ex/9706006](#)]; A. A. Aguilar et al. [LSND Collaboration], *Phys. Rev. D* 64, 112007 (2001) [[arXiv:hep-ex/0104049](#)].

[19] O. L. G. Peres and A. Y. Smirnov, *Nucl. Phys. B* 599, 3 (2001) [[arXiv:hep-ph/0011054](#)].

[20] M. Sorel, J. Conrad and M. H. Shaevitz, *Phys. Rev. D* 70, 073004 (2004) [[arXiv:hep-ph/0305255](#)].

[21] I. E. Stockdale et al., *Phys. Rev. Lett.* 52, 1384 (1984).

[22] F. Dydak et al., *Phys. Lett. B* 134, 281 (1984).

[23] Y. Declais et al., *Nucl. Phys. B* 434, 503 (1995).

[24] M. A. pollonio et al., [[arXiv:hep-ex/0301017](#)].

[25] B. Ambrosius et al. [KARMEN Collaboration], *Phys. Rev. D* 65, 112001 (2002) [[arXiv:hep-ex/0203021](#)].

[26] P. A. Stier et al. [NOMAD Collaboration], *Phys. Lett. B* 570, 19 (2003) [[arXiv:hep-ex/0306037](#)]; D. G. Gibin, *Nucl. Phys. Proc. Suppl.* 66, 366 (1998); V. Valuev [NOMAD Collaboration], SPHERES entry Prepared for International Europhysics Conference on High-Energy Physics (HEP 2001), Budapest, Hungary, 12–18 Jul 2001.

[27] M. M. Altoni, T. Schwetz, M. Tortola and J. W. F. Valle, *New J. Phys.* 6, 122 (2004) [[arXiv:hep-ph/0405172](#)].

[28] V. D. Barger, Y. B. Dai, K. Whisnant and B. L. Young, *Phys. Rev. D* 59, 113010 (1999) [[arXiv:hep-ph/9901388](#)].

[29] B. Kayser, [[arXiv:hep-ph/0211134](#)].

[30] P. Brønmark, *Markov chains: Gibbs fields, Monte Carlo simulation, and queues*, Springer, New York, 1999.

[31] N. M. Metropolis, A. W. Rosenbluth, M. N. Rosenbluth, A. H. Teller and E. Teller, *J. Chem. Phys.* 21, 1087 (1953).

[32] M. Honda, T. Kajita, K. Kasahara and S. Midorikawa, *Phys. Rev. D* 70, 043008 (2004) [[arXiv:astro-ph/0404457](#)].

[33] M. C. Gonzalez-Garcia and M. M. Altoni, *Phys. Rev. D* 70, 033010 (2004) [[arXiv:hep-ph/0404085](#)].

[34] M. M. Altoni, T. Schwetz and J. W. F. Valle, *Phys. Lett. B* 518, 252 (2001) [[arXiv:hep-ph/0107150](#)].

[35] A. A. Aguilar-Arevalo et al. [MINIBOONE Collaboration], *Phys. Rev. D* 66, 033008 (2002) [[arXiv:hep-ph/0109053](#)].

[36] D. Casper, *Nucl. Phys. Proc. Suppl.* 112, 161 (2002) [[arXiv:hep-ph/0208030](#)].

[37] M. M. Altoni, T. Schwetz, M. A. Tortola and J. W. F. Valle, *Nucl. Phys. B* 643, 321 (2002) [[arXiv:hep-ph/0207157](#)].

[38] A. Strumia, *Phys. Lett. B* 539, 91 (2002) [[arXiv:hep-ph/0201134](#)].

[39] W. Grimus and T. Schwetz, *Eur. Phys. J. C* 20, 1 (2001) [[arXiv:hep-ph/0102252](#)].

[40] S. Hannestad, *Prog. Part. Nucl. Phys.* 57, 309 (2006) [[arXiv:astro-ph/0511595](#)].

[41] K. Abazajian, N. F. Bell, G. M. Fuller and Y. Y. Y. Wong, *Phys. Rev. D* 72, 063004 (2005) [[arXiv:astro-ph/0410175](#)].

[42] G. Gelmini, S. Palomares-Ruiz and S. Pascoli, *Phys. Rev. Lett.* 93, 081302 (2004) [[arXiv:astro-ph/0403323](#)].